

Nanostructures of liquid crystal phases in mixtures of bent-core and rod-shaped molecules

S. H. Hong,¹ R. Verduzco,³ J. T. Gleeson,¹ S. Sprunt,¹ and A. Jáklí²

¹*Department of Physics, Kent State University, Kent, Ohio 44242, USA*

²*Liquid Crystal Institute, Kent State University, Kent, Ohio 44242, USA*

³*Rice University, 6100 Main Street, MS-362, Houston, Texas 77008, USA*

(Received 4 March 2011; published 9 June 2011)

We report small angle x-ray scattering (SAXS) studies of isotropic, nematic, and smectic mesophases formed by binary mixtures of bent-core (BC) and rod-shaped (RS) molecules. While optical studies indicate that the components are fully miscible, SAXS reveals fascinating structures that are consistent with segregation on a nanoscopic scale. We find that tilted smectic clusters, which have been previously reported in both the nematic and isotropic states of the pure BC materials, are also present in mixtures with up to 50 wt% of the RS compound; this is consistent with previous dielectric and flexoelectric studies on such mixtures. Unexpectedly in this concentration range the clusters are present in the isotropic and in the induced smectic phase range, as well as throughout the nematic phase. The results in the smectic phase also reveal complex layering phenomena, providing important insight into the interaction between bent and rod-shaped molecules. These studies will be crucial in the design of promising new functional nanomaterials.

DOI: [10.1103/PhysRevE.83.061702](https://doi.org/10.1103/PhysRevE.83.061702)

PACS number(s): 61.30.-v, 42.70.Df, 87.59.-e

I. INTRODUCTION

Mixing two or more different chemical compounds is a common procedure in liquid crystal science. The goals are typically to tailor material properties [1], to obtain specific phases with wide range of temperature, or to achieve materials with large anisotropy and/or low viscosity that are important for many applications. Studies of mixtures may also reveal important physical properties of the constituent molecules. Studying mixtures is not only useful for traditional, rod-shaped (RS) liquid crystals, but also for bent-core liquid crystals (BCLCs) [2]. BCLCs are of primary scientific interest due to their unique combination of polarity and chirality [3]; they also exhibit useful characteristics for electro-optical [4] or electromechanical [5] applications. With a few exceptions [6,7], pure bent-core compounds have liquid crystal phases above room temperature [8], which limits their utility for many applications. Mixtures of bent-core and rod-shaped molecules (as summarized recently in Ref. [9]) generally show interesting properties, such as a decrease of the helical pitch in the cholesteric phase [10,11], induction of antiferroelectric order in smectics [10,12], nanoseparation [13,14], or the broadening of the mesophase temperature range [15–17] by up to 50 °C and extending it to near room temperature.

On the other hand, small angle x-ray scattering (SAXS) experiments on pure BC materials revealed the presence of short-range correlated, tilted smectic clusters in the nematic and isotropic phases at temperatures well above the nematic-smectic transition [18,19], and further that this clustering exists in the isotropic and nematic phases even in the absence of any lower temperature smectic phase [20]. The size of these clusters does not show the temperature dependence one would expect from pretransitional effects, and therefore are qualitatively different from “cybotactic groups,” which are well known in materials having an underlying smectic phase. The clusters can be understood as a result of broken local translational symmetry of the nematic phase due to the close packing of bent-shaped molecules; this mechanism can explain a number of unusual properties of bent-core nematics [5,21,22].

The aim of this paper is to investigate the nature of molecular clustering in binary mixtures of bent-core (BC) and rod-shaped (RS) molecules and to find out how the short-range structure depends on the concentration of RS compounds. The nature of the tilted smectic clusters and related aspects of the nanostructure of the mixtures will be also discussed.

II. EXPERIMENTS AND RESULTS

The BC compound used in our study is 4-chloro-1,3-phenylene bis[4-(10-decenyloxy) benzoyloxy] benzoate (abbreviated ClPbis10BB) with phase sequence $I-74\text{ }^\circ\text{C}-N-50\text{ }^\circ\text{C}-Cr$. Its liquid crystalline properties have been extensively investigated [5,18,20–23]; end to end, the molecular length (L_{BC}) is about 45 Å. The RS compound, 4-*n*-octyloxyphenyl 4-*n*-hexyloxybenzoate (6OO8), phase sequence $I-87\text{ }^\circ\text{C}-N-46\text{ }^\circ\text{C}-SmC-38\text{ }^\circ\text{C}-Cr$, was chosen because its structure is similar to one arm of the BC compound; its molecular length (L_{RS}) is about 26 Å. We prepared mixtures with five different concentrations: with 16.3, 32.3, 48.3, 65.6, and 83.6 wt% of the RS compound. These mixtures have phase sequences $I-77\text{ }^\circ\text{C}-N-56\text{ }^\circ\text{C}-SmC_A-40\text{ }^\circ\text{C}-Cr$; $I-81\text{ }^\circ\text{C}-N-63\text{ }^\circ\text{C}-SmC_A-37\text{ }^\circ\text{C}-Cr$; $I-84\text{ }^\circ\text{C}-N-65\text{ }^\circ\text{C}-SmC_A-24\text{ }^\circ\text{C}-Cr$; $I-85\text{ }^\circ\text{C}-N-66\text{ }^\circ\text{C}-SmC_A-17\text{ }^\circ\text{C}-Cr$; $I-86\text{ }^\circ\text{C}-N-63\text{ }^\circ\text{C}-SmA-57\text{ }^\circ\text{C}-SmC_A-38\text{ }^\circ\text{C}-Cr$, respectively. Previous optical studies [17] of these mixtures found no evidence of immiscibility at all concentrations studied. The mixtures were filled into 1-mm-diameter quartz x-ray tubes, which were then mounted into a custom-built aluminum cassette that allowed x-ray detection with $\pm 13.5^\circ$ angular range. The cassette fits into a standard hot stage (Instec model HCS402) that allowed temperature control with $\pm 0.01\text{ }^\circ\text{C}$ precision. The stage also included two cylindrical neodymium iron boron magnets that supplied a magnetic induction of $B = 1.5\text{ T}$ at the position of the x-ray capillary. The magnetic field direction is perpendicular to the incident x-ray beam. Two-dimensional (2D) SAXS images were recorded on a Princeton Instruments 2084×2084 pixel array charge-coupled device (CCD) detector in the

X6B beamline at the National Synchrotron Light Source (NSLS). The beamline was configured for a collimated beam ($0.2 \text{ mm} \times 0.3 \text{ mm}$) at energy 16 keV (0.775 \AA). Prior to the SAXS measurements, the alignment of the nematic director under the influence of the magnetic field was checked by polarizing optical microscopy and found to be uniform over the scattering volume. Details of the experimental conditions are the same as used for the studies of the pure compounds; see Ref. [20].

Pure compounds: Before addressing the mixtures, it is important to recap previous SAXS results on the pure compounds:

(i) In their isotropic phase, both compounds exhibit diffuse ring patterns in the small angle scattering. In the BC material, the d spacing corresponding to the ring is $d \approx 32 \text{ \AA}$ and the positional correlation length is $\xi \approx 46 \text{ \AA}$. These results are consistent with an isotropic distribution of *tilted* smectic clusters of about $90\text{--}100 \text{ \AA}$ size [24]. In rod-shaped material, the d spacing associated with the small angle diffraction ring is $d \approx 27 \text{ \AA}$ and the correlation length $\xi = 30 \text{ \AA}$ are both comparable to L_{RS} ; this indicates that in this compound the intermolecular correlations can be straightforwardly explained by McMillan's excluded volume effect [25].

(ii) In the RS compound, as the temperature is decreased below the clearing point and through the nematic range, the intensity and narrowness of a fourfold lobe pattern increases dramatically as the SmC transition temperature is approached. This behavior is completely consistent with classic pretransitional critical phenomena, specifically the development and growth (in both size and lifetime) of fluctuations in the SmC ordering, so-called "cybotactic groups." In sharp contrast, the BC compound behaves both qualitatively and quantitatively differently. On cooling into its nematic phase, the diffuse ring pattern in the BC material transforms first into two arcs, and as temperature is lowered, this evolves into to a four-lobed scattering pattern. However, there is no significant increase in the intensity or the narrowness of these lobes as the temperature ranges from the clearing point throughout the entire nematic range. The lobe pattern in this case is indicative of short-range SmC order, but this is not caused by the proximity to a smectic phase, does not behave critically, and cannot be attributed to cybotactic groups. Smecticlike "clusters" is the term that is most commonly used to refer to these structures.

With the behavior of the pure compounds in mind, we turn to the SAXS patterns exhibited by mixtures. We distinguish between two regimes: BC rich (RS wt% $< 40\%$) and RS rich (RS wt% $> 40\%$).

BC-rich range: Typical 2D x-ray patterns from our BC-RS binary mixtures are shown in Fig. 1 for the 16.3 wt% and 32.3 wt% RS concentrations. The top row of Fig. 1(a) shows that in the isotropic phase and near the T_{NI} in the nematic phase ($T_{NI} - T = \Delta T < 4^\circ\text{C}$), the 2D SAXS is similar to that observed in the pure BC material reported in [17]; an isotropic diffuse ring above T_{NI} and a flattening of this ring just below T_{NI} . As the temperature is further decreased, a diffuse four-lobe pattern forms (over a wide temperature range, $5^\circ\text{C} < \Delta T < 20^\circ\text{C}$). These lobes are centered at scattering vector, $q \sim 0.19 \text{ \AA}^{-1}$, corresponding to a d spacing of 33 \AA . This is considerably shorter than the L_{BC} molecules but larger than L_{RS} . The peak centers are oriented about

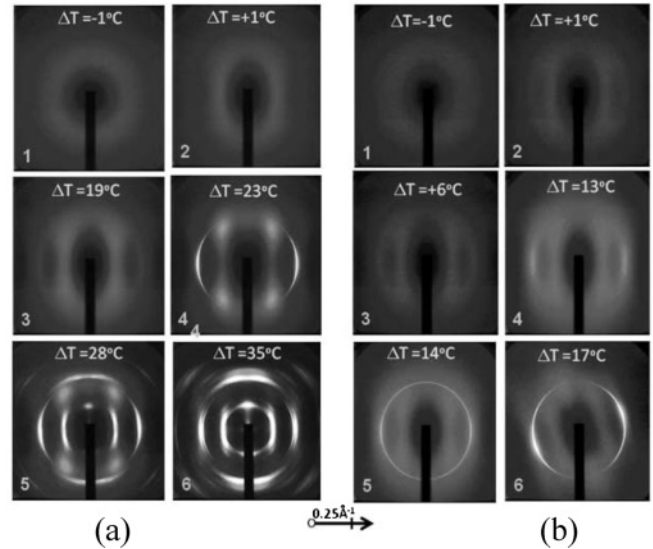


FIG. 1. Representative SAXS patterns and their proposed director and layer structures. (a) The mixture with 16.3 wt% of RS molecules; (b) 32.3 wt% of RS in BC compound at selected temperatures.

$42^\circ\text{--}45^\circ$ off the horizontal, which is the applied magnetic field direction. Since $33 \text{ \AA} \sim L_{BC} \cos 43^\circ$ we interpret these lobes as indicating the existence of smectic clusters having short-range positional order and tilted with respect to the direction of average molecular alignment. At lower temperatures ($\Delta T = 22^\circ\text{C}$) a pair of arcs, which are narrowly centered at a specific value of $q = 22 \text{ \AA}^{-1}$ (corresponding to a d spacing of $d = 29 \text{ \AA}$) appear; this indicates the presence of long-range smectic order. The peak intensity of these arcs is centered along the horizontal axis, but they extend to very large angles off this axis, indicating that the smectic-layer normal is only weakly established by the orientation of the nematic director. It is further important to note that the layer spacing is significantly smaller than that of the SmC clusters deduced from the four-lobe pattern.

At still lower temperatures [e.g., ΔT as low as $\sim 23^\circ\text{C}$ in 16.3 wt% RS; see Fig. 1(a4)] the four lobes sharpen somewhat and new, narrow, untilted-smectic arcs (corresponding to a d spacing of $\sim 43 \text{ \AA}$) develop with layer normal along the magnetic field. Just below this regime, at $\Delta T = 28^\circ\text{C}$ and slightly above the crystallization, additional features develop: wide peaks appear at $q = 0.22 \text{ \AA}^{-1}$ (corresponding to a d spacing $\sim 28 \text{ \AA}$) with layer normal almost perpendicular to the original smectic layer direction, and a pair of diffuse spots appear at $q = 0.14 \text{ \AA}^{-1}$ (corresponding to d spacing $\sim 45 \text{ \AA}$), with layer normal perpendicular to the magnetic field; only one of these is not obscured by the beamstop in Fig. 1(a5). Below $\Delta T = 35^\circ\text{C}$ the material crystallizes.

In the 32.3-wt% mixture the four lobe pattern is qualitatively the same [see Figs. 1(b2)–1(b4)] as is seen for higher temperatures in the 16.3-wt% mixture. The four lobes are more diffuse, which we attribute to increased RS content. This also leads to relatively stronger smectic peaks below $\Delta T \sim 13^\circ\text{C}$; at $\Delta T > 17^\circ\text{C}$ one sees a gradual rotation of the whole pattern without the appearance of the extra peaks.

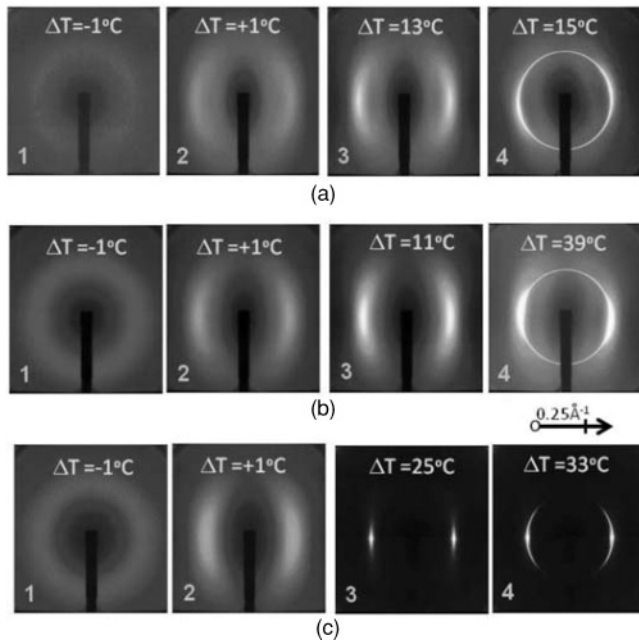


FIG. 2. 2D small angle x-ray patterns in the rod-shaped molecules dominated concentration ranges. (a) 48.3 wt%; (b) 65.6 wt%; (c) 83.6 wt% of rod-shaped molecules. Note that in the low temperatures of (c) the illumination time is much shorter than in all other pictures, because the smectic peaks are so intense they would saturate the detector.

RS-rich range: Typical 2D x-ray patterns at the RS rich range (48.3, 65.6, and 83.6 wt% of RS molecules) are shown in Figs. 2(a4) and 2(b4). Just as for the 32.3-wt% concentration, in the intermediate 48.3 and 65.6 wt% mixtures the smectic peaks are rotated slightly off the magnetic field direction at lower temperatures of the SmC_A phase ranges. This rotation does not occur for the 83-wt% RS concentration; in this case, about 25 °C below the $I-N$ transition a well correlated smectic layer structure forms along the applied field direction.

III. DISCUSSION

As is demonstrated above, mixtures of RS and BC compounds exhibit remarkable nanostructures that are not found in either pure compound. Most striking of all, the SAXS patterns indicate the presence of phase segregation, while optical microscopy studies [17] show the compounds fully miscible. Therefore the segregation is limited to length scales below optical wavelengths. Below, we present some proposed mechanisms for these observations. For this purpose, it is convenient to consider three different temperature ranges: nematic, nematic-smectic, and complex smectic. The first range shows no long-range smectic order, the second has a single long-range-ordered smectic peak, and the third shows multiple smectic peaks. The notation and legend for our model structures are shown in Fig. 3(a). One remarkable feature of all intermediate-range concentrations (except the 16.3- and the 83.6-wt% concentrations) is the overall tilt of the structures near the crystalline transition. Although x-ray experts find such effects frequently, and they usually attribute this to a

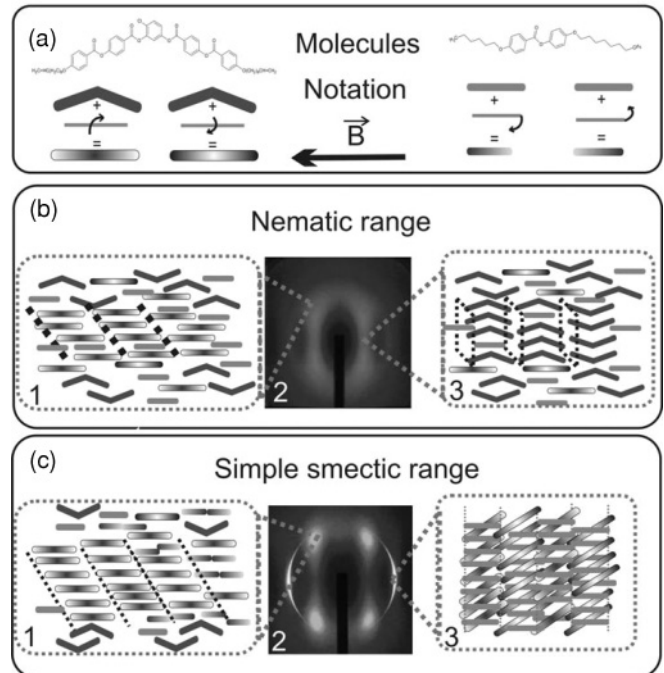


FIG. 3. (a) Molecular structures and their notation. (b) and (c) Representative 2D SAXS patterns and their corresponding proposed nanostructures in the nematic and simple smectic ranges. Dotted lines indicate the layering. A thicker dotted line indicates a shorter correlation length.

surface memory effect [26], we do not fully understand this effect, and we believe such rotations deserve further and deeper studies. In this work we rather concentrate on the results specific to our materials, and leave this issue for the future.

Of all mixtures studied, 16.3 wt% of RS shows the widest variety of nanostructures. In the nematic range the 2D SAXS patterns do not show microsegregation; the short-range correlated tilted smectic clusters are very similar to those observed for the pure BC material [20]. This may indicate that there may be a higher concentration of BC inside clusters than outside. Tilted smectic clusters lead to the best-defined peaks in the SAXS pattern [see Fig. 3(b1)]. However, these peaks are somewhat smeared out and are connected by a band of SAXS intensity that corresponds to a longer d spacing. We interpret this to mean that the long axes of the BC molecules are well coupled to the magnetic field, but, they are fairly free to rotate about the field direction. This leads to a small population of normal smectic clusters (with $d \sim L_{BC} \sim 45$ Å) as shown in Fig. 3(b3).

In the nematic-smectic range, which occurs at lower temperatures, we see the first indications of microphase segregation. Specifically, concurrently with SAXS that is characteristic of a nematic structure containing tilted smectic clusters with short-range order, we also observe long-range untilted smectic order with layer normal preferentially aligned along the magnetic field [Fig. 3(c2)]. The layer periodicity of the smectic component is about 29 Å, which is midway between that of the tilted clusters (33 Å) and L_{RS} . As the magnetic Fredericksz transition in the BC molecules occurs at higher fields than in the RS molecules [27], it is reasonable

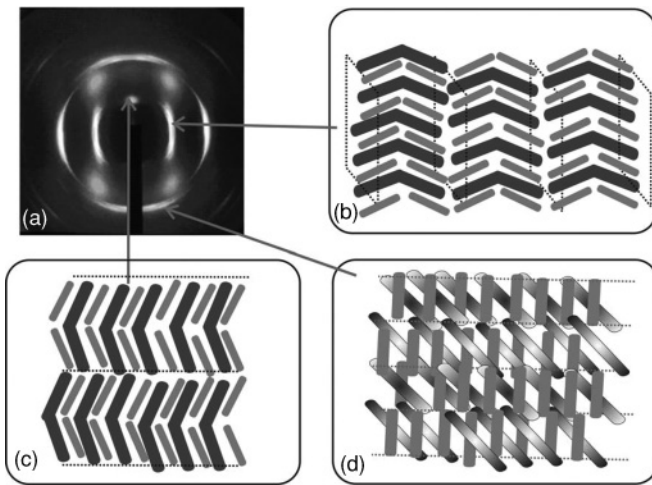


FIG. 4. 2D SAXS profile and its model cartoons at the low temperature range (5°C above the crystal transition).

to assume that at low temperatures the microphase segregated volumes richer in RS molecules could be more susceptible for magnetic alignment, leading to a smectic phase with layers normal to the magnetic field. The observed SAXS pattern suggests a local structure where the BC molecules are tilted either by more than 45° and/or there is an interdigitation between the BC molecules. This latter structure can be achieved with a little energy increase if the arms of the neighbor BC compounds are synclinic, which is obtained if the average dipoles along the kink are opposite. Such a director and layer structure is illustrated in Fig. 3(c3).

At low temperatures near the smectic-crystal transition a complex smectic structure forms (see Fig. 4). First we discuss the additional peaks indicating nontilted smectic layering with d spacing ~ 45 Å. This structure basically evolved from the short-range structure shown in Fig. 3(b3), so we think it has the same layering, but now with long-range correlation. Note that this is a polar arrangement where arms of the neighbor BC molecules tilt with respect to each other explaining why they do not interpenetrate. The deviation of this smectic arc from a circle also indicates that the layers are somewhat tilted with respect to the x-ray beam as indicated in Fig. 4(b).

Simultaneously with the formation of this secondary smectic ring, a relatively sharp peak with the same (~ 45 Å) spacing, but with layer normal perpendicular to the magnetic field, appears. This peak above the beam stop can be explained as a result of local positional molecular fluctuations that will lead to the appearance of layers perpendicular to the magnetic field [see Fig. 4(c)]. The q value of the peak and of the secondary layers are the same, because the tilt angle is $\theta \sim 45^\circ$, i.e., $\sin\theta = \cos\theta$. To explain the formation of the stripes almost perpendicular to the primary smectic layers we note that in these directions diffuse stripes have already been seen in the nematic phase. These correspond to those clusters formed already in the isotropic phase where the director was perpendicular to the magnetic field, since the magnetic field had no effect on director orientation in the isotropic range. In the nematic phase they still were present, because there the

director is basically perpendicular to the field. In this case a symmetry breaking is needed to rotate the director, so it would require a threshold magnetic field. The director fluctuation is decreasing at lower temperatures, and would completely halt upon the transition to the smectic phase, thus leading to layers with director perpendicular to the magnetic field. The slight decrease of the periodicity of these smectic domains indicate either an additional tilt [perhaps “leaning” as seen in Fig. 4(d)], or some layer modulation. In any case, the further fine splitting of the stripes, and the fact that they do not appear at $\Delta T = 23^\circ\text{C}$ together with the primary SmA-type layers, indicate that they represent a different smectic structure. Details of this structure could be the subject of further studies.

The persistence of the four lobe diffuse scattering—i.e., the scattering from short-range correlated uniformly tilted (SmC) clusters—into a phase, whose SAXS pattern implies long-range smectic correlations, is one of the most interesting elements of our study. A closer look at the 2D x-ray pattern illustrates that the correlation length in this range is increased to about 100 Å, indicating about 20-nm cluster size that is about twice that in the nematic range. The layer spacing of these clusters is midway between that of the primary (larger q) and secondary (smaller q) layers that corresponded to antipolar and polar layers, respectively. Consequently we may argue that the clusters may contain both antipolar and polar domains, and/or tilt angles with larger and smaller than 45° . Also it is important to note that none of the long-range layer structure penetrates into the χ range of the clusters. For these reasons we hypothesize that the clusters contain much fewer RS molecules than the rest of the sample and they form segregated nanodomains. They disappear only once the material has crystallized as shown at $\Delta T = 35^\circ\text{C}$ of Fig. 1(a). Future freeze-fracture TEM studies are underway with a goal to clarify exactly this question.

What is the significance of these clusters? They persist up to about 40 wt% of RS (see Fig. 1). They disappear at higher RS concentrations and only SmA- or SmCA-type two lobe patches exist (see Fig. 2); The concentration range where the tilted smectic clusters are observed coincides with the range where large linear electromechanical effect [28], anomalous second harmonic generation (SHG) signal [29], and low frequency dielectric mode [23] are observed. As we argued above, tilted (synclinic) smectic domains of BC materials have either antipolar or polar structures [3]. Since antipolar domains are unlikely to cause observable contributions to linear electromechanical effects, SHG signals, or low frequency dielectric modes, we conclude that the uniformly tilted smectic clusters must be at least partially polar in accordance with the observations analyzed above.

IV. SUMMARY

We have investigated the nature of molecular clustering in binary mixtures of bent-core (BC) and rod-shaped (RS) molecules to find out how the short-range structure depends on the concentration of RS compounds. We have shown that in these mixtures, the tilted smectic clusters disappear at about 1:1 wt% concentration, which is similar to the concentration where

one observes a critical weakening of the flexoelectric effect [5] and also of certain low frequency dielectric modes [23]. We also found that in the range where the BC molecules are the majority component, the tilted smectic clusters persist even in the smectic phase that occurs in the mixtures and disappear only upon the transition to the crystalline phase. Our results can be consistently explained assuming the formation of smectic layers both with polar and antipolar layer arrangement, which seem to coexist in the tilted smectic clusters as well.

ACKNOWLEDGMENTS

The work was supported by the NSF under Grant No. DMR-0964765. Materials were provided by R. J. Twieg, J. C. Williams, and K. Fodor-Csorba. Use of the National Synchrotron Light Source, Brookhaven National Laboratory, was supported by the US Department of Energy, Office of Science, Office of Basic Energy Sciences, under Contract No. DE-AC02-98CH10886. We acknowledge useful discussions with R. Pindak and E. DiMasi at BNL.

-
- [1] See, G. Pelzl, S. Diele, K. Ziebart, W. Weissflog, and D. Demus, *Liq. Cryst.* **8**, 765 (1990), and reference therein.
- [2] T. Niori, T. Sekine, J. Watanabe, T. Furukawa, and H. Takezoe, *J. Mater. Chem.* **6**, 1231 (1996).
- [3] D. R. Link, G. Natale, R. Shao, J. E. MacLennan, N. A. Clark, E. Kőrblova, and D. M. Walba, *Science* **278**, 1924 (1997).
- [4] A. Jákli, *Liq. Cryst. Today* **11**, 1 (2002).
- [5] J. Harden, B. Mbanga, N. Eber, K. Fodor-Csorba, S. Sprunt, J. T. Gleeson, and A. Jákli, *Phys. Rev. Lett.* **97**, 157802 (2006).
- [6] J. Matraszek, J. Mieczkowski, J. Szydłowska, and E. Gorecka, *Liq. Cryst.* **27**, 429 (2000).
- [7] S. Rauch, C. Selbmann, P. Bault, H. Sawade, G. Heppke, O. Morales-Saavedra, M. Y. M. Huang, and A. Jákli, *Phys. Rev. E* **69**, 021707 (2004).
- [8] G. Pelzl and W. Weissflog, in *Thermotropic Liquid Crystals: Recent Advances*, edited by A. Ramamoorthy, Chap. 1 (Springer, New York, 2007), pp. 1–43.
- [9] N. V. Madhusudana, *Liq. Cryst.* **36**, 1173 (2009).
- [10] E. Gorecka, M. Cepic, J. Mieczkowski, M. Nakata, H. Takezoe, and B. Zeks, *Phys. Rev. E* **67**, 061704 (2003).
- [11] M. Nakata, Y. Takanishi, J. Watanabe, and H. Takezoe, *Phys. Rev. E* **68**, 041710 (2003).
- [12] E. Gorecka, M. Nakata, J. Mieczkowski, Y. Takanashi, K. Ishikawa, J. Watanabe, H. Takezoe, S. H. Eichhorn, and T. M. Swager, *Phys. Rev. Lett.* **85**, 2526 (2000).
- [13] K. Takekoshi, K. Ema, H. Yao, Y. Takanishi, J. Watanabe, and H. Takezoe, *Phys. Rev. Lett.* **97**, 197801 (2006).
- [14] C. Zhu, D. Chen, Y. Shen, C. D. Jones, M. A. Glaser, J. E. MacLennan, and N. A. Clark, *Phys. Rev. E* **81**, 011704 (2010).
- [15] R. Prathibha, N. V. Madhusudana, and B. K. Sadashiva, *Science* **288**, 2184 (2000).
- [16] M. W. Schröder, S. Diele, G. Pelzl, N. Pancenko, and W. Weissflog, *Liq. Cryst.* **29**, 1039 (2002).
- [17] G. G. Nair, C. A. Bailey, S. Taushanoff, K. Fodor-Csorba, A. Vajda, Z. Varga, A. Bóta, and A. Jákli, *Adv. Mater.* **20**, 3138 (2008).
- [18] O. Francescangeli, V. Stanic, S. I. Torgova, A. Strigazzi, N. Scaramuzza, C. Ferrero, I. P. Dolbnya, T. M. Weiss, R. Berardi, L. Muccioli, S. Orlandi, and C. Zannoni, *Adv. Funct. Mater.* **19**, 1 (2009).
- [19] N. Vaupotic, J. Szydłowska, M. Salamonczyk, A. Kovarova, J. Svoboda, M. Osipov, D. Pocięcha, and E. Gorecka, *Phys. Rev. E* **80**, 030701 (2009).
- [20] S. H. Hong, R. Verduzco, J. Williams, R. J. Twieg, E. DiMasi, R. Pindak, A. Jákli, J. T. Gleeson, and S. Sprunt, *Soft Matter* **6**, 4819 (2010).
- [21] C. Bailey, K. Fodor-Csorba, J. T. Gleeson, S. N. Sprunt, and A. Jákli, *Soft Matter* **5**, 3618 (2009).
- [22] C. Bailey, K. Fodor-Csorba, R. Verduzco, J. T. Gleeson, S. Sprunt, and A. Jákli, *Phys. Rev. Lett.* **103**, 237803 (2009).
- [23] P. Salamon, N. Éber, Á. Buka, J. T. Gleeson, S. Sprunt, and A. Jákli, *Phys. Rev. E* **81**, 031711 (2010).
- [24] O. Francescangeli, M. Laus, and G. Galli, *Phys. Rev. E* **55**, 481 (1997).
- [25] W. L. McMillan, *Phys. Rev. A* **6**, 936 (1972).
- [26] E. DiMasi (private communication).
- [27] T. Ostapenko, C. Zhang, J. T. Gleeson, and A. Jákli (submitted to *Phys. Rev. E*).
- [28] A. Jákli, M. Chambers, J. Harden, M. Majumbar, R. Teeling, J. Kim, Q. Li, G. G. Nair, N. Éber, K. Fodor-Csorba, J. T. Gleeson, and S. Sprunt, *Proc. SPIE-Int. Soc. Opt. Eng.* **6911**, 691105 (2008).
- [29] S. H. Hong, A. Jákli, J. Gleeson, S. Sprunt, and B. Ellman, *Phys. Rev. E* **82**, 041710 (2010).